Dense growth of multiply-twinned star-shaped molybdenum particles by atmospheric H_2/Ar microplasma jet

Yoshiki Shimizu,* Kenji Koga, Takeshi Sasaki, and Naoto Koshizaki

Setup of the apparatus and details of deposition process

Figure S1(a) depict the schematic illustration of the apparatus. An alumina tube (inner diameter 800 μm, outer diameter 1.2 mm) was used as a nozzle for microplasma generation and connected to a stainless-steel tube for the plasma gas to flow in. Mo wire (200 μm in diameter) for source material was inserted into the nozzle to 1 mm from the nozzle exit. A 5 mm long, five-turn solenoid coil made of brass was wound around the zone, 1 mm from the nozzle exit. One end of this coil was connected to a ultra-high-frequency (UHF, 450 MHz) power supply via a matching circuit, while the other end was left floating.

The substrate for deposition (Mo, W, MgO , Al_2O_3 plates) was placed 1 to 3 mm away from the nozzle exit. Ar gas, mixed with less than 4%H_2 (below lower explosion limit concentration of H_2 (4 vol.%) in air), was introduced at flow rate of up to 1000 sccm and UHF power of up to 30 W was supplied to the coil through a matching circuit. The microplasma was stably generated in the nozzle and jetted out from the nozzle exit into the ambient air (microplasma jet). The molybdenum wire inserted in the nozzle was evaporated by the generated microplasma, and the resultant active species are transported downstream and condensed (deposited) on a localized area (about 1 mm diameter) on the substrate (Figurer S1(b)). The deposition area was directly irradiated and heated with the microplasma jet (Figure S1(c)).

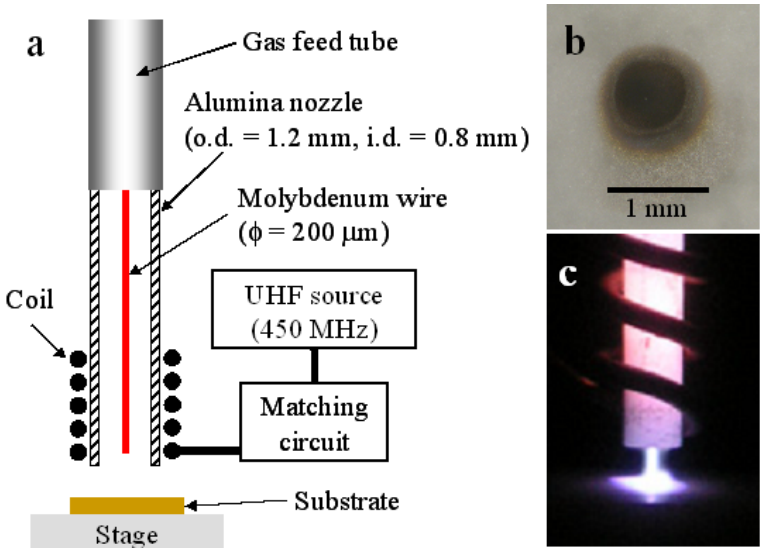

Figure SI 1 (a) Schematic illustration of the apparatus employed in this study. (b) Optical microscope image of a typical deposit. (c) Photograph that depicts the deposition process.

Detailed characterization of an individual particle with TEM and TED to prove the star-shaped particles as multiply twinned particles.

Figures SI 2(a) and (b) present a TEM image of a single s-Mo-MTP whose height exceeds 100 nm, taken along the <110> direction, and the corresponding SAED pattern. The SAED pattern roughly consists of five <110> zone axis patterns of f.c.c. structure. The details will be explained below, with the HRTEM observations. Figure SI2 (c) is an HRTEM image of part α (as indicated in Fig. SI2 (a)). In this image, two lattice images are observed across the centerline of the protrusion (broken line). Lattices above and below the line correspond to the {111} planes (*d*-spacing = 2.3 Å) and {200} planes (*d*-spacing = 2.0 Å) of f.c.c. Mo, respectively. This angular relationship between the {111} and the {200} planes, as seen in Fig. SI2 (c), is impossible in real space for the <110> zone of an individual f.c.c. crystal, and thus we can conclude that the protrusions have a twin structure and that the center line is a twin plane.

Figure SI 2(d) illustrates a possible reciprocal lattice-point pattern corresponding to part α, based on the HRTEM image in (c) and the SAED pattern in (b). This pattern is the superposition of two <110> zone axis pattern, and the black and white circles reveal the patterns corresponding to each crystal unit (subunit) above and below the twin plane, respectively. An analysis of this pattern reveals that the twin plane is {111}. The in-line arrangements of some spots appearing in the SAED pattern (indicated by white-arrowed continuous lines in Fig. SI2 (b)) were attributed to this twin structure.

At the next protrusion (indicated as β in Fig. SI 2(a)), the same twin structure was observed (Fig. SI 2(e)). It should be noted that the direction of the {200} plane (*d*-spacing = 2.0 Å) is the same as was observed in Fig. SI 2(c). Consequently, the {200} lattices in Figs. SI 2(c) and (e) must be in an individual subunit. A possible reciprocal lattice-point pattern taken from this protrusion, based on the HRTEM image in (e) and the SAED pattern in (b), is illustrated in Fig. SI 2(f). The pattern delineated by the white circles, corresponding to the right-side subunit in Fig. SI 2(e), is exactly the same as the white-circle pattern in Fig. SI 2(d), and the black circles reveal the pattern of the left-side subunit. Their superposition aligns the spots as indicated by the white-arrowed broken line in Fig. SI 2(b).

Further characterizations of other protrusions turned out to be almost the same as those for α and β, indicating that the s-Mo-MTP is roughly divided into five subunits, as seen in Fig. SI 2(g), with two neighboring subunits having a relationship of twins across the {111} plane, that is, a multiply twinned particle (MTP). The central angle of regions A, B, C, and D, marked in Fig. SI 2 (g), was measured to be 70 to 71 degrees, almost corresponding to angle formed by two intersecting {111} planes in the <110> zone of the f.c.c. structure, while angle E was definitely determined to be 76 to 80 degrees, which includes an extra 5 to 10 degrees due to the misfit. In order to explain how to

relax this misfit in the MTP, Iijima introduced a small-angle grain boundary in one individual subunit,[25] while Saito reported distortion in some subunits.[26] In fact, the SAED pattern in Fig. SI 2 (b) was composed of six <110> zone axis patterns. Of these, two patterns other than those corresponding to A, B, C, and D subunits were attributed to region E; their superposition, based on the SAED pattern in Fig. SI 2(b), is illustrated in Fig. SI 2(h). As revealed by the splitting of two {111} type diffraction spots in Fig. SI 2(b) (indicated by arrow heads), two <110> zone axis patterns are superposed on each other with a rotation angle of 8 degrees about the zone axis. The pattern indicated by the black circles has a twin relationship with the pattern from subunit A across the {111} plane. However, due to the angular relation, this pattern cannot make a twin relationship across the {111} plane with a pattern from subunit D. Instead, the pattern illustrated by the white circles has a twin relationship with the pattern from subunit D across the {111} plane. Consequently, we assumed that an additional grain boundary was introduced between two protrusions in subunit E to relax the misfit, as indicated by the broken line in Fig. SI 2(g). We attempted to directly observe this boundary by HRTEM, but this was impossible due to the excessive depth, corresponding to the height of the s-Mo-MTP.

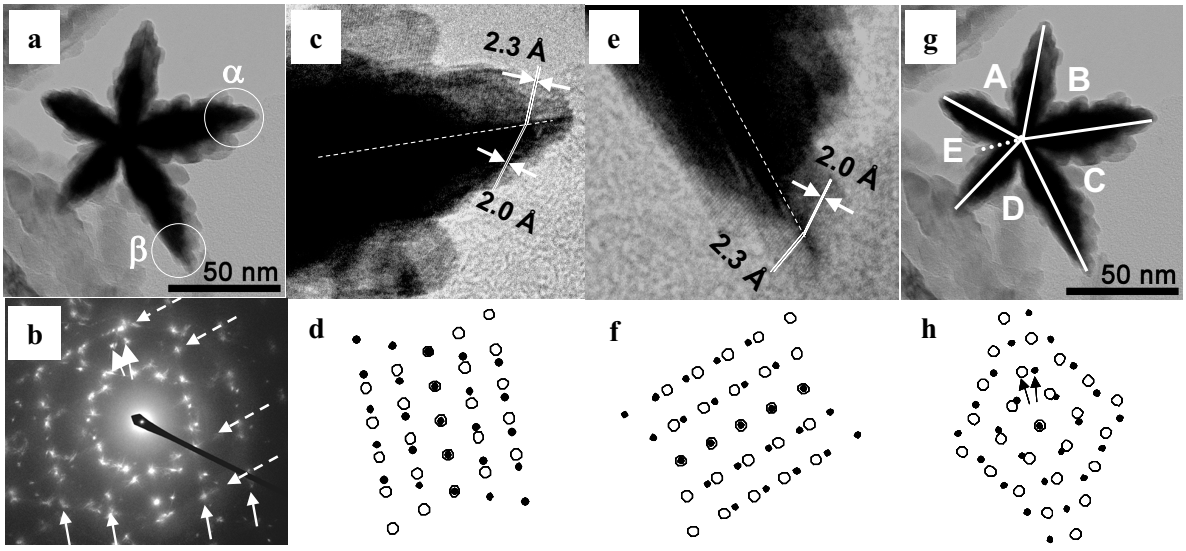

Figure SI 2 Detailed structural characterization of an individual s-Mo-MTP by TEM and SAED.

Evidence suggesting that the root-sides of the s-Mo-MTPs were buried by a layer composed of irregular spherical particles.

As seen in Figs. 6 (a, b), the growing s-Mo-MTPs appear to form a conical shape on the layer composed of irregular spherical particles. This shape thus seems to differ from those observed with SEM (Fig. 1(c)) and TEM (Fig. 4(a)). This difference can be explained by the following observations.

We pressed conductive tape onto the top of the deposit, in which mature s-Mo-MTPs were densely formed, as illustrated in Fig. SI 3(a), peeled it off (Fig. SI3 (b)) and then observed the substrate and s-Mo-MTPs attached on the adhesive face of the tape.

Figure SI 3(d) depicts a deposit on the substrate after removal of the mature s-Mo-MTPs (as explained schematically in Fig. SI 3(c). Irregular spherical particles remained embedded on the substrate, and crater-like parts appeared.

In contrast, Fig.SI 3(f) shows s-Mo-MTPs attached on the adhesive face of the tape, thus revealing the bottom side of the s-Mo-MTPs (as explained schematically in Fig. SI 3(e)). Acute tips were typically observed, and no particles with wide base as seen in Fig. 6(a-b) were observed. Accordingly, we can conclude that s-Mo-MTPs as seen in Fig. 1(c) was located in the crater parts formed in the deposit composed of irregular spherical particles, as simply illustrated in Fig. 7.

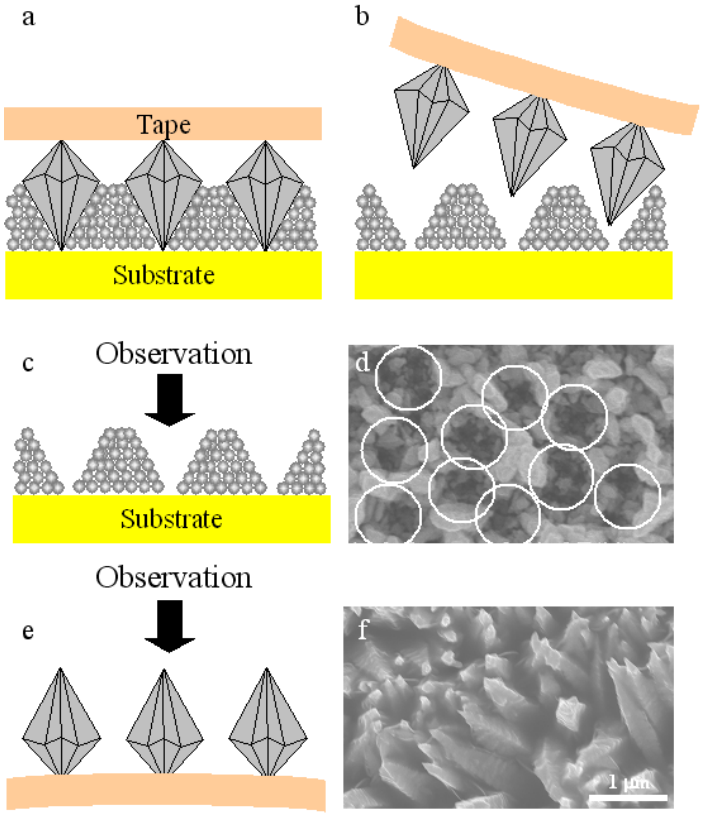

Figure SI 3 Explanation drawing of peel-off of s-Mo-MTPs, and their observations from top and bottom sides by SEM.

Morphological change of the deposited particles with varying gap distance

The importance of the gap distance was evident in these depositions. Even with both the substrate temperature and the gas flow rate in suitable ranges, s-Mo-MTPs (Fig. SI 4 (a)) were formed only with a 1-mm gap distance. At 2 mm, leaf-like particles were densely but randomly deposited (Fig. SI 4 (b)). Meanwhile, growing leaf-like particles were sparsely formed in the dense nanoparticle deposits (Fig. SI 4 (c)).

Table 1 Conditions for depositions shown in Figs. SI 4

Figure No.	Gas flow rate (ccm)	Gap distance (mm)	Temperature at the back of the substrate(℃)	Growth of star-shaped Mo	Note
Fig. SI4(a)	500	1	370	Yes	s-Mo-MTPs were densely formed.
Fig. SI4(a)	500	2	375	No	Leaf-like grains were formed densely but randomly.
Fig. SI4(c)	500	3	330	No	Irregular spherical particles were densely deposited.

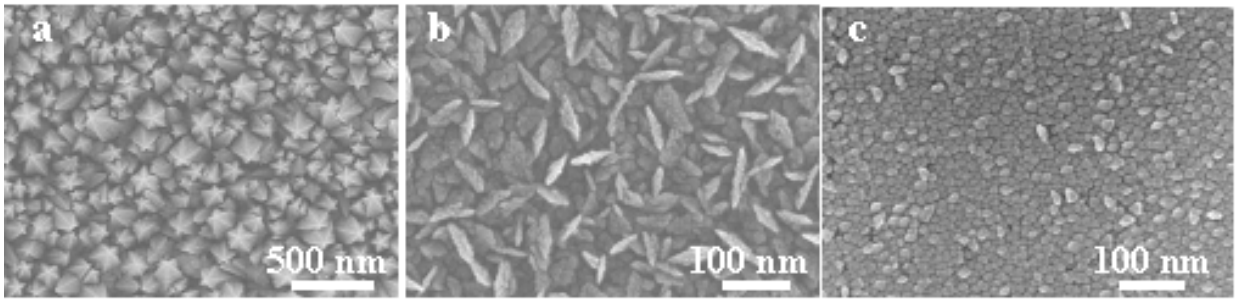

Figure SI 4 Morphological change in deposits on Mo plate with varying gap distance by SEM observation. (a) 1 mm, (b) 2 mm, and (c) 3 mm.

Growth model of star-shaped particles on a substrate

Cheng et al reported the preparation of star-shaped TiN particles by CVD performed in low pressure chamber (Ref 22: H. E. Cheng et al, *Scripta Materialia,* 1996, **35**, 113). The growth model in this case is illustrated in Figure SI 5(a). The nuclei grow mainly upward (indicated by blue arrow) and laterally along five twin boundaries (indicated by red arrows) to form s-MTP with wide bases that are roughly conical in shape.

On the other hand, in case of s-Mo-MTP reported in this paper, the base growth, as indicated by red arrows, was hindered by obstacle particles around the nuclei (Fig. 8(a)). Thus, the base area remains small and the growth direction is limited to upward (indicated by dashed lines in Fig. 8(a)). Consequently, the formed s-Mo-MTP has top-heavy morphology (Fig. 8 (b-c)).

After s-Mo-MTPs are densely formed on the substrate as illustrated in Fig. 8(c), growth direction of the s-Mo-MTPs is limited only upward direction due to steric hindrance (Fig. SI 5(b)). Actually, we can obtained the particles, as seen in Fig. SI 5(c), in deposition for longer deposition time (more than 1 hour)

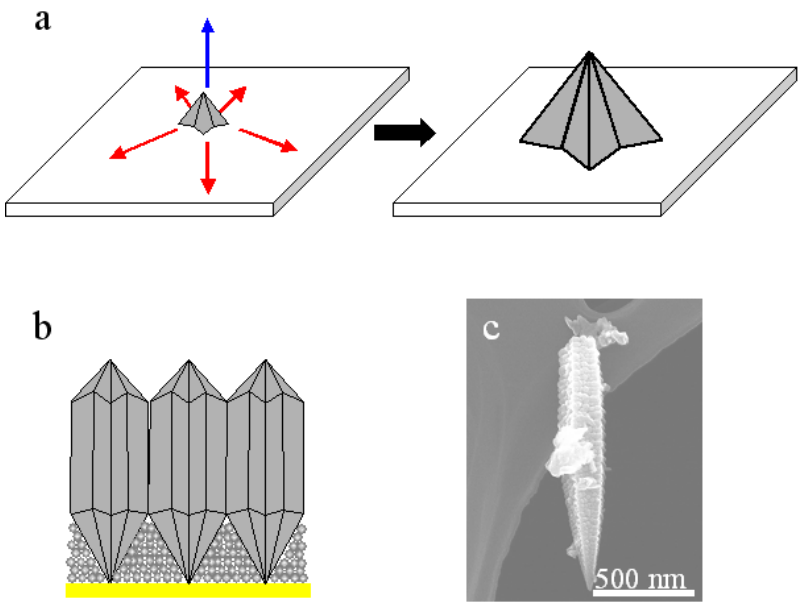

Figure SI 5 (a) Growth model of star-shaped TiN particles formed by low-pressure CVD process, reported by Cheng et al. (b, c) Schematic illustration of s-Mo-MTPs formed in deposition for longer time, and SEM observation of the resultant s-Mo-MTP (side view).